

Transport methods for energetic particles

Wu Hong-Lu

(KRUG Life Sciences, Houston, TX 77058, USA)

Yang Chui-Hsu

(NASA Johnson Space Center, Houston, TX 77058, USA)

Abstract In order to estimate radiation risk assessment for astronaut's radiation safety in space activities, transport codes for high energy particles have been created. Two of the transport methods, perturbation and Green function methods, for high energy particles are reviewed in this paper, and some of the calculated results with the perturbation method are presented. Finally, the low energy transport in the regard of the biological effects by low energy ions is also briefly discussed

Keywords Energetic particles, Transport codes, Radiation safety, Biological effect

1 Introduction

The development of transport codes for high energy particles has been a constant effort in the regard of astronaut's radiation safety in space activities.^[1] The three major radiation sources in space environment are galactic cosmic rays (GCR), trapped protons and particles due to large solar particle events. Trapped protons in the Van Allen belt are the dominating radiation source for lower earth orbit (LEO) flights. The energy of the trapped protons is usually less than 1000 MeV. In free space environment, however, astronauts are bombarded

constantly by GCR and occasionally by the particles from large solar particle events. Although the energy of the particles from solar particle events are relatively low, their intensity is so high that exposure to the radiation from a single event may exceed the exposure limit. GCRs, on the other hand, have lower intensities, but the high energy and heavy components of the particles may cause more damage to the biological systems. Thus, both GCR and the radiation due to large solar particle events can be fatal for long duration missions such as mission to Mars. The space radiation environment is shown in Fig.1.

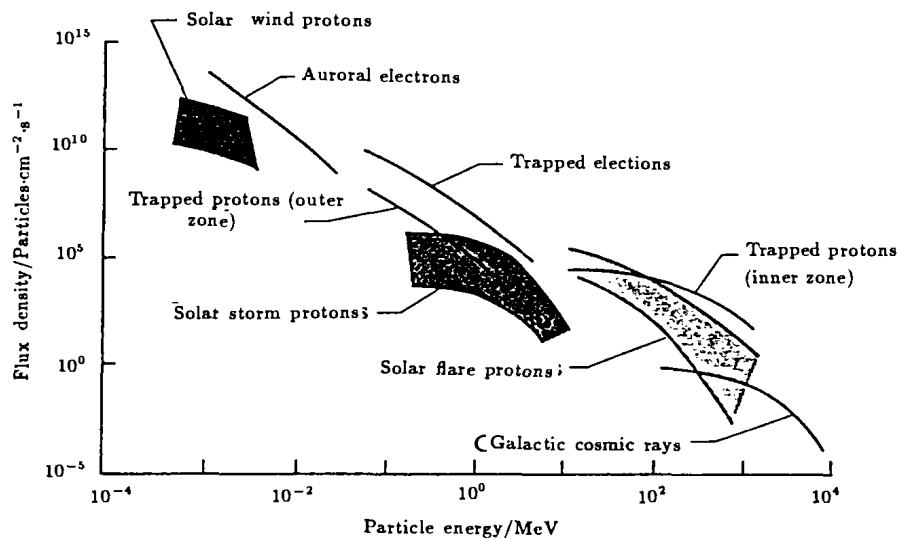


Fig.1 Space radiation environment

Transport codes have been used for radiation risk assessment for previous space flights and making risk predictions for future missions.^[2] The purpose of a transport code is to solve the following Boltzmann equation:

$$\begin{aligned} & \left[\Omega \cdot \nabla - \frac{1}{A_j} \frac{\partial}{\partial E} S_j(E) + \sigma_j(E) \right] \phi_j(\chi, \Omega, E) \\ & = \sum_k \int dE' d\Omega' \sigma_{jk}(E, E', \Omega, \Omega') \phi_k(\chi, \Omega', E') \end{aligned} \quad (1)$$

where $\phi_j(\chi, \Omega, E)$ is the flux of ions of type j with atomic mass A_j at location χ . The particles move along the direction Ω with energy E in the unit of MeV/u. In Eq.(1), $\sigma_j(E)$ is the macroscopic cross section, $S_j(E)$ is the linear energy transfer (LET), and $\sigma_{jk}(E, E', \Omega, \Omega')$ is the creation cross section for j type particle with energy E and direction Ω by the collision of type k particle of energy E' and direction Ω' . The continuous slowing down approximation has been made in arriving at Eq.(1).

For energy below the threshold of the nuclear reaction, the term on the right-hand side and the last term on the left-hand side in Eq.(1) disappear and the solution to the Boltzmann equation is straightforward. We will discuss briefly some of the results for low energy transport in plant seed in Sec.5. The main purpose of the present paper is to review some of the numerical algorithms developed in recent years for high energy ions.

Solutions to the Boltzmann equation with nuclear reaction terms can be obtained analytically only in some special cases. In most cases, the solution relies on the use of computers. Over the year, a number of computer codes have been developed, including the Monte Carlo codes^[3] and codes based on other algorithms. In the next three sections, we will review two of the numerical methods developed in recent years and present some of the results for space applications.

It should be noted that for the biological damage by energetic particles, the quantities of interest are the absorption dose

$$D = \sum_k \int dE' \phi_k(\chi, \Omega', E') S_k(E') \quad (2)$$

and dose equivalent

$$H = \sum_k \int dE' \phi_k(\chi, \Omega', E') S_k(E') Q \quad (3)$$

where Q is the quality factor and is a function of LET. In this paper, the quality factors from ICRP-60^[4] are used.

2 Perturbation method^[5]

The straight-ahead approximation may reduce the computing time drastically. This approximation is usually valid for high energy transport and is adopted in the perturbation method discussed in this section. With the approximation, the transport process becomes one-dimensional and Eq.(1) may be written as

$$\begin{aligned} & \left[\frac{\partial}{\partial \chi} - \frac{1}{A_j} \frac{\partial}{\partial E} S_j(E) + \sigma_j \right] \phi_j(\chi, E) \\ & = \sum_k \int dE' \sigma_{jk}(E, E') \phi_k(\chi, E') \end{aligned} \quad (4)$$

The following equation with simpler notations will be used to illustrate the perturbation methods. Detailed solution for Eq.(4) may be derived similarly. The simplified equation is

$$\begin{aligned} & \left[\frac{\partial}{\partial \chi} - \frac{\partial}{\partial E} S(E) + \sigma \right] \phi(\chi, E) \\ & = \int_E^\infty f(E, E') \phi(\chi, E') dE' \end{aligned} \quad (5)$$

The transformations

$$r = \int_0^E dE' / S(E') \quad (6)$$

$$\Psi(\chi, r) = S(E) \phi(\chi, E) \quad (7)$$

$$\bar{f}(r, r') = S(E) f(E, E') \quad (8)$$

allow Eq.(5) to be written as

$$\begin{aligned} & \left[\frac{\partial}{\partial \chi} - \frac{\partial}{\partial r} + \sigma \right] \phi(\chi, r) \\ & = \int_r^\infty \bar{f}(r, r') \phi(\chi, r') dr' \end{aligned} \quad (9)$$

The solution of the differential-integral equation (9) can be written as

$$\Psi(\chi, r) = e^{-\sigma\chi}\Psi(0, r + \chi) + \int_0^\chi dz e^{-\sigma z} \int_{r+z}^\infty dr' \bar{f}(r + z, r') \Psi(x - z, r') \quad (10)$$

with the boundary condition given by

$$\Psi(0, r) = S(E)\phi(0, E) \quad (11)$$

A numerical algorithm^[5] for Eq.(10) is found by noting that

$$\Psi(\chi + h, r) = e^{-\sigma\chi}\Psi(\chi, r + h) + \int_0^h dz e^{-\sigma z} + \int_{r+z}^\infty dr' \bar{f}(r + z, r' + z) \Psi(\chi + h - z, r' + z) \quad (12)$$

The integral term is of the order of $O(h)$ (where h is the step size) and thus

$$\Psi(\chi + h - z, r) = e^{-\sigma(h-z)}\Psi(\chi, r + h - z) + O(h - z) \quad (13)$$

Substituting Eq.(13) into Eq.(12), one has

$$\Psi(\chi + h, r) \approx e^{-\sigma\chi}\Psi(\chi, r + h) + e^{-\sigma h} \int_0^h dz \int_{r+z}^\infty dr' \bar{f}(r + z, r' + z) \Psi(\chi, r' + h) \quad (14)$$

to terms (h^2). Eq.(14) can be shown^[1] to be accurate for distances such that $\sigma h \ll 1$ and may be used to propagate the spectrum at some point χ to the spectrum at $\chi + h$. Therefore, one may begin at the boundary ($\chi = 0$) and propagate the solution to an arbitrary interior point. Eq.(14) is useful for continuous spectra.

In laboratory experiments, the particles are mostly mono-energetic and the boundary has a discrete spectrum given by

$$\Psi(0, E) = \delta(E - E_0) \quad (15) \quad \text{while the continuous term satisfies}$$

$$\Psi_c(\chi + h, r) = \exp(-\sigma h)\Psi_c(\chi, r + h)$$

$$+ \int_0^h dz \exp(-\sigma z) \int_r^\infty dr' \bar{f}(r + z, r' + z) [\Psi_s(\chi + h - z, r' + z) + \Psi_c(\chi + h - z, r' + z)] \quad (18)$$

Following the same procedure as for continuous spectra, one has

$$\Psi_c(\chi + h - z, r) = e^{-\sigma(h-z)}\Psi_c(\chi, r + h - z) + O(h - z) \quad (19)$$

With the use of Eq.(17), the solution for the continuous component may be approximated as

$$\begin{aligned} \Psi_c(\chi + h, r) \approx & \exp(-\sigma h) [\Psi_c(\chi, r + h) + \exp(-\sigma\chi)\bar{F}(r, h, r_0 - \chi - h)] \\ & + \exp(-\sigma h) \int_r^\infty dr' \bar{F}(r, h, r') \Psi_c(\chi, r' + h) \end{aligned} \quad (20)$$

where

$$F(r, h, r') = \int_0^h dz f(r + z, r') = F_c[\varepsilon(r + h), E'] - F_c(E, E') \quad (21)$$

Then

$$\Psi(0, r) = \delta(r - r_0) \quad (16)$$

when discrete spectra are present at the boundary, the solution is divided into singular and continuous components labeled by Ψ_s and Ψ_c , respectively. The solution of the singular component is

$$\Psi_s(\chi, r) = \exp(-\sigma\chi)\delta(r + \chi - r_0) \quad (17)$$

In Eq.(21), $\varepsilon(r)$ is the energy for range r and

$$F_c(E, E') = \int_0^E f(E, E') dE \quad (22)$$

Eqs.(17, 20) are used to propagate the spectrum for mono-energetic particle from a distance χ to $\chi + h$.

3 Results with the perturbation method

In this section, we present some of the calculated results with the BRYNTRN^[6] and HZETRN^[7] codes based on the above algorithm for the space radiation environment in lower earth orbits. In LEO, trapped protons in the Van Allen belt are the major radiation source and the energy spectrum for the trapped protons in the orbit at 270 n.m. altitude, 28.5 degree inclination and solar maximum activities is shown in Fig.2. Although GCRs are one of the major concerns in free space, only the high energy GCRs are capable to penetrate through the geomagnetic field to LEO, and their contribution to the exposure is usually small at low inclination orbits. Shown in Fig.3 is the dose and dose equivalent as a function of shield thickness

of tissue. The tissue is assumed to be protected by a 5 g/cm² aluminum, which represents the shield of spacecraft. One of the risks due to the chronic exposure to the space radiation is the development of leukemia. The radiation exposure to the blood-forming-organs (BFO) is directly responsible for leukemia and may be estimated by the exposure at 5 cm depth of tissue. Compared with the exposure limit of 25 rem in 30 d for BFO, the risk for a short LEO space flight is below the limit.

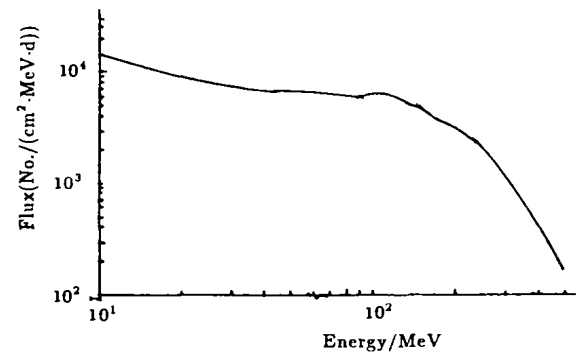


Fig.2 Trapped proton spectrum in 28.5 degree orbit at 270 n.m. altitude and solar maximum activities

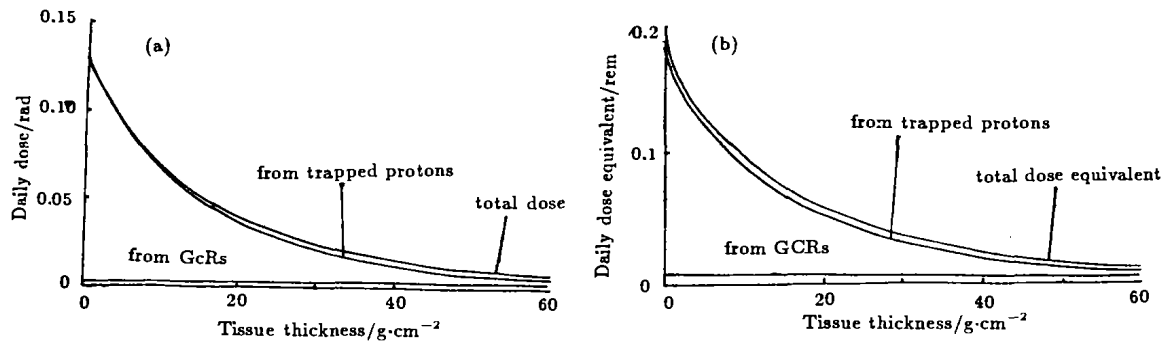


Fig.3 Daily dose and dose equivalent as a function of tissue shield thickness in 270 n.m. altitude and 28.5 degree inclination orbit at solar max. The tissue is behind a 5 g/cm² Al shield

4 Green function method^[8]

A more recent approach to the solution of the Boltzmann equation is based on the Green function, and is outlined in this section.

The Boltzmann equation (Eq.1) in the first section may be written formally as

$$\mathbf{B}\phi = \mathbf{P}\phi \quad (23)$$

The solution of Eq.(23) can be written as

$$\phi = \phi_0 + \mathbf{B}^{-1}\mathbf{P}\phi \quad (24)$$

where ϕ_0 is the solution of the homogeneous equation. A propagation matrix Green function \mathbf{G}_0 is defined as

$$\phi = \mathbf{G}_0\phi_B + \mathbf{B}^{-1}\mathbf{P}\phi \quad (25)$$

where ϕ_B is the boundary condition and

$$\mathbf{B}\mathbf{G}_0 = 0 \quad (26)$$

The Neumann series solution of Eq.(25) can be written as

$$\begin{aligned} \phi = & \mathbf{G}_0\phi_B + \mathbf{B}^{-1}\mathbf{P}\mathbf{G}_0\phi_B + \mathbf{B}^{-1}\mathbf{P}\mathbf{B}^{-1}\mathbf{P}\mathbf{G}_0\phi_B \\ & + \dots \end{aligned} \quad (27)$$

The complete Green function is defined as

$$\phi = \mathbf{G}\phi_B \quad (28)$$

and can be expanded by the series

$$\begin{aligned} \mathbf{G} = & \mathbf{G}_0 + \mathbf{B}^{-1}\mathbf{P}\mathbf{G}_0 + \mathbf{B}^{-1}\mathbf{P}\mathbf{B}^{-1}\mathbf{P}\mathbf{G}_0 \\ & + \dots \end{aligned} \quad (29)$$

The above series can also be written as

$$\mathbf{G} = \mathbf{G}_0 + \mathbf{B}^{-1}\mathbf{P}\mathbf{G} \quad (30)$$

Thus, the Green function \mathbf{G} also satisfies

$$\mathbf{B}\mathbf{G} = \mathbf{P}\mathbf{G} \quad (31)$$

In component form, Eq.(31) is written as

$$\left[\Omega \cdot \nabla - \frac{\partial}{\partial E} \bar{S}_j(E) + \sigma_j(E) \right] G_{jm}(\chi, \Omega, E, E_0) = \sum_k \int dE' d\Omega' \sigma_{jk}(E, E', \Omega, \Omega') G_{km}(\chi, \Omega', E', E_0) \quad (32)$$

where $\bar{S}_j(E)$ is the change in E per unit distance, and E now denotes the energy per nucleon. Thus, the Green function is the solution of Eq.(32) subject to the boundary condition

$$G_{jm}(0, \Omega, E, E_0) = \delta_{jm} \delta(\Omega - \Omega', E - E_0) \quad (33)$$

The solution to the Boltzmann equation can be expressed in terms of the Green function as

$$\phi_j(E, \Omega, \chi) = \sum_m \int dE' d\Omega' d\Gamma G_{km}(\chi - \Gamma, \Omega - \Omega', E', E_0) f_m(E', \Omega', \Gamma) \quad (34)$$

where $f_m(E', \Omega', \Gamma)$ is the incident flux at the boundary.

In one-dimension (straight-ahead approximation), Eq.(32) becomes

$$\left[\frac{\partial}{\partial \chi} - \frac{\partial}{\partial E} \bar{S}_j(E) + \sigma_j \right] G_{jm}(\chi, E, E_0) = \sum_k \int dE' \sigma_{jk}(E, E') G_{km}(\chi, E', E_0) \quad (35)$$

Under the velocity conservation approximation^[1], Eq.(35) can be written as

$$\left[\frac{\partial}{\partial \chi} - \frac{\partial}{\partial E} \bar{S}_j(E) + \sigma_j \right] G_{jm}(\chi, E, E_0) = \sum_k \sigma_{jk} G_{km}(\chi, E, E_0) \quad (36)$$

The Green function in Eq.(36) may be solved with the following non-perturbative technique. This technique uses the generator equation given by

$$\left[\frac{d}{d\chi} + \sigma_j \right] g_{jm}(\chi) = \sum_k \sigma_{jk} g_{km}(\chi) \quad (37)$$

This equation is subject to the boundary condition $g_{jm}(0) = \delta_{jm}$. It can be shown^[8] that

g_{jm} satisfies the following recurrence relation

$$g_{jm}(\chi) = \sum_k g_{jk}(\chi - y) g_{km}(y) \quad (38)$$

The value of g_{jm} at any distance χ may be found non-perturbatively using Eq.(38). It can be shown^[8] that the Green function in Eq.(36), expressed in terms of g_{jm} , is given by

$$G_{jm}(\chi, r_j, r'_m) = \exp(-\sigma_j \chi) \delta_{jm} \delta(\chi + r_j - r'_m) + \frac{\sigma_{jm}}{\Delta(1)} g(j, m) + \frac{g_{jm}(\chi) - g(j) \delta_{jm} - \sigma_{jm} g(j, m)}{\Delta(2)} \quad (39)$$

where r_j is defined in Eq.(6). In Eq.(39),

$$g(j) = \exp(-\sigma_j \chi) \quad (40)$$

$$g(j, m) = \frac{g(j) - g(m)}{\sigma_m - \sigma_j} \quad (41)$$

$$\Delta^{(1)} = \chi \left(\frac{V_m}{V_j} - 1 \right) \quad (42)$$

$$\Delta^{(2)} = \begin{cases} \chi(V_m/V_j - 1) & (V_m > V_k > V_j) \\ \chi(V_k/V_j - 1) & (V_k > V_m > V_j) \\ \chi(V_m/V_j - \frac{V_k}{V_j}) & (V_m > V_j > V_k) \end{cases} \quad (43)$$

and $V_j = Z_j^2/A_j$.

5 Low energy transport

For low energy particles, the solution to the Boltzmann equation is straightforward because the terms for nuclear reactions vanish. The range and the energy deposited are then completely determined by the stopping power $S(E)$. Since Professor Yu Zeng-liang and coworkers have observed mutations in rice seed irradiated with low energy nitrogen ions, we calculated the range of nitrogen ions in starch, $(C_6H_{10}O_5)_n$, and present the results in Fig.4. A similar result for protons on cellulose nitrate can be found in Ref.[9].

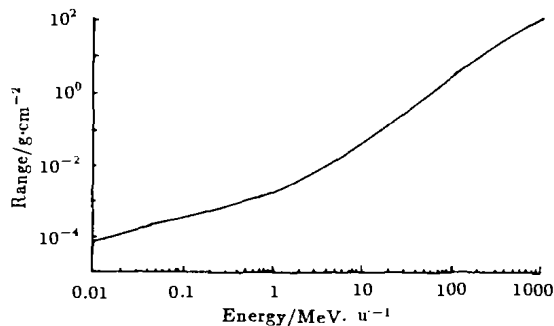


Fig.4 Range of nitrogen in starch as a function of energy

6 Summary

Two of the transport methods for high energy particles are reviewed in the present paper. Like most of the numerical algorithms in solving partial differential equations, the perturbative technique discussed in Sec.2 is limited by the step size and the number of the steps. For large

depth, smaller steps must be taken to limit the numerical error. As a result, the computational time increases. Care must also be taken to apply the perturbative method to mono-energetic particle beams because the energy grids in the vicinity of the energy of the primary particle have to be small enough to ensure the accuracy of the computation. The Green function method reviewed in Sec.4 is a non-perturbative method, and thus a more accurate and efficient method.

The accuracy of the solution to the Boltzmann equation depends also on the accuracy of the cross sections of the nuclear reactions. The uncertainties may be introduced by the lack of experimental data for certain reaction channels and certain ranges of energy. Other errors in the computer codes are due to the simplifications and assumptions made on the nuclear reactions. The subject of nuclear reaction models constitutes another major effort in the development of high energy transport codes, and is not discussed in this paper.

References

- 1 Wilson J W, Townsend L W, Schimmerling W *et al.* Transport methods and interactions for space radiation, NASA RP-1257. Texas: NASA Johnson Space Center, 1991
- 2 Wu H, Atwell W, Hardy A C *et al.* SAE Tech Paper, Ser 932211, Proceedings of 23rd International Conference on Environmental Systems, 1993
- 3 Alsmiller R G. Nucl Sci and Eng, 1967; 27(2):158
- 4 1990 Recommendations of the International Commission on Radiological Protection. ICRP Publ 60. New York: Pergamon Press Inc, 1991
- 5 Wilson J W, Townsend L W, Ganapol B *et al.* Nuclear Sci and Eng, 1988; 99(3):223
- 6 Wilson J W, Townsend L W, Nealy J E *et al.* NASA TP-2887, Texas: NASA Johnson Space Center, 1989
- 7 Wilson J W, Chun S Y, Badavi F F *et al.* NASA. TP-3146. Texas: NASA Johnson Space Center, 1991
- 8 Wilson J W, Costen R C, Shinn J L *et al.* NASA TP-3311. Texas: NASA Johnson Space Center, 1993
- 9 Janni J F. Atom Data and Nucl Data Tables, 1982; 27:147